Pergamon

*Int. J. Heat Mass Transfer.* Vol. 39, No. 4, pp. 717–724, 1996

0017-9310/96 $15.00+0.00

0017-9310(95)00172-7

# Semi-analytical solution of thermal energy storage system with conjugate laminar forced convection

YUWEN ZHANG and AMIR FAGHRI†

Department of Mechanical Engineering, University of Connecticut, Storrs, CT 06269-3139, U.S.A.

(*Received* 29 *December* 1994 *and in final form* 15 *May* 1995)

**Abstract**—A thermal energy storage system with a hollow cylinder of Phase Change Material (PCM) was studied semi-analytically. The melting of the PCM was solved by using an integral approximate method, and heat transfer in the container wall was treated as a radial one dimensional conduction problem. The forced convective heat transfer inside the tube was solved by an analytical method, which was coupled with the heat conduction in the PCM and the container wall. The results show that the laminar forced convective heat transfer inside the tube never reached the fully developed state, even for a very long tube. For a transfer fluid of moderate Prandtl number, the laminar forced convective transfer inside the tube must be solved simultaneously with the phase change of the PCM.

## 1. INTRODUCTION

Interest in utilizing clean energy sources, such as solar energy, is growing because of environmental considerations. However, due to its periodic nature, a thermal energy storage device is needed. The latent heat thermal energy storage system is a very effective device for this purpose, because the Phase Change Material (PCM) can absorb or release a large amount of heat during its melting or solidification process. Figure 1 shows a typical configuration of the latent heat thermal energy storage system. The system consists of a hollow cylinder of PCM with a transfer fluid flowing inside the inner tube for the purpose of heat exchange.

Heat transfer in the thermal energy storage system, similar to Fig. 1, is a conjugate phase-change/convection problem. Hsu and Sparrow [1] presented a closed form analytical solution for freezing adjacent to plane wall cooled by forced convection. Sparrow and Hsu [2] numerically solved the two-dimensional (2D) freezing on the outside of a coolant-carrying tube. Shamsundar [3] presented a closed form solution of the same problem by ignoring the sensible heat and axial conduction of the PCM. The agreement between Shamsundar's analytical solution [3] and Sparrow and Hsu's numerical solution [2] were very good for the case with Stefan number $Ste = 0$. Shamsundar and Rooz [4] presented a numerical solution of the same problem using a finite element method. Charach *et al.* [5] studied the problem for small Stanton number by using a perturbation method. In all of the above investigations, the thickness of the PCM outside the tube was considered to be infinite, which is unrealistic from the view point of the practical application. Inside the tube, they assumed that the convective heat transfer coefficient was uniform and constant.

A PCM model similar to that in Fig. 1 was studied by Solomon *et al.* [6]. In their model, the PCM outside the tube was considered to be a finite thickness, which differed with refs. [2–5]. A finite difference formulation with the Kirchhoff temperature was used to calculate the internal energy, temperature and the location of solid–liquid interface. Cao and Faghri numerically simulated the performance of this thermal energy storage system with laminar forced convection [7] and turbulent forced convection in the tube [8]. In their analyses, the change of phase of the PCM and the transient forced convective heat transfer were solved simultaneously as a conjugate problem. Due to the primary concern of a space-based application, a liquid metal with low Prandtl number was used as the transfer fluid in ref. [7]. Forced convective heat transfer inside the tube occurred in the thermal and hydrodynamic entry region. It was determined that if a steady state fully developed heat transfer correlation was used to calculate the heat transfer coefficient inside the tube, a significant error would be introduced. Thus, the transient forced convective heat transfer in the tube must be solved simultaneously with the change of phase of the PCM.

Recently, a Solar Receiver Unit (SRU), similar to Fig. 1, was studied by Bellecci and Conti [9]. However, the outer wall of the system was not perfectly adiabatic since radiative losses were assumed. The SRU collected the solar irradiation focused by a concentrator on the outer cylinder. In order to check Cao and Faghri's [7] conclusions, Bellecci and Conti [9] also

† Author to whom correspondence should be addressed.

## NOMENCLATURE

| | |
|---|---|
| $c$ | specific heat [J kg$^{-1}$ K$^{-1}$] |
| $D$ | inside diameter of the tube [m] |
| $Fo$ | Fourier number, $\alpha_p t/r_i^2$ |
| $G_n$ | constant in equations (21) and (22) |
| $h$ | local convection heat transfer coefficient [W m$^{-2}$ K$^{-1}$] |
| $H$ | latent heat of melting [J kg$^{-1}$] |
| $k$ | thermal conductivity [W m$^{-1}$ K$^{-1}$] |
| $K$ | dimensionless thermal conductivity, $k/k_p$ |
| $L$ | length of the tube [m] |
| $M$ | section number of the tube along the axial direction |
| $N$ | section number of the PCM along the axial direction |
| $Nu$ | local Nusselt number, $hD/k_f$ |
| $Pe$ | Peclet number, $U_m D/\alpha_f$ |
| $r$ | coordinate along the radial direction [m] |
| $R$ | dimensionless coordinate along the radial direction, $r/r_i$ |
| $s$ | solid–liquid interface radius [m] |
| $S$ | dimensionless solid–liquid interface radius, $s/r_i$ |
| $Ste$ | Stefan number, $c_p(T^0_{in} - T^0_m)/H$ |
| $T^0$ | temperature [K] |
| $T$ | dimensionless temperature, $(T^0 - T^0_m)/(T^0_{in} - T^0_m)$ |
| $t$ | time [s] |
| $u$ | velocity [m s$^{-1}$] |
| $U_m$ | average velocity [m s$^{-1}$] |
| $x$ | coordinate along the axial direction [m] |
| $X$ | dimensionless coordinate along the axial direction, $x/D$. |

Greek symbols

| | |
|---|---|
| $\alpha$ | thermal diffusivity [m$^2$ s$^{-1}$] |
| $\lambda_n$ | eigenvalues |
| $\rho$ | density [kg m$^{-3}$]. |

Subscripts

| | |
|---|---|
| b | bulk |
| f | transfer fluid |
| i | inside radius of the tube, or grid point in axial direction |
| in | inlet |
| o | outer wall of thermal energy storage system |
| p | PCM |
| w | container wall or inner surface of container wall |
| wo | outer surface of container wall. |

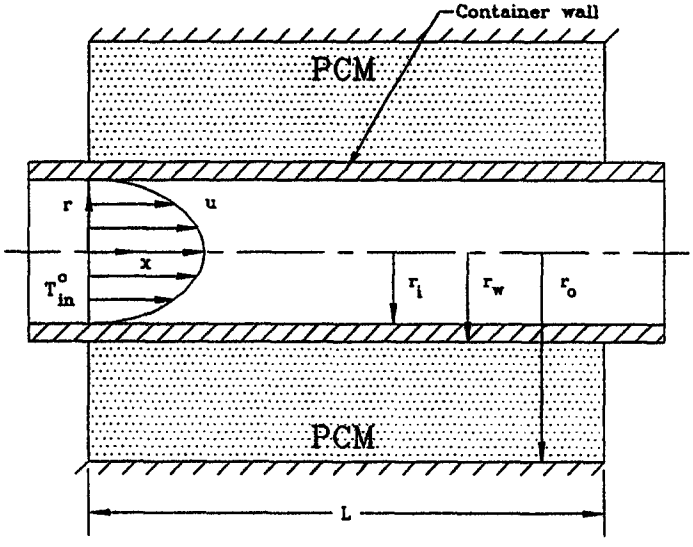


Fig. 1. Schematic of PCM energy storage model with laminar flow inside the tube.

calculated the melting front position for an adiabatic outer wall. The convective heat transfer coefficient was quoted from the steady state numerical results of Chen and Chiou [10] for liquid metals in the thermal and hydrodynamic entry length regions. It can be shown that the agreement between their results and Cao and Faghri's [7] results was quite satisfactory. Therefore, Bellecci and Conti concluded that the con-

vective heat transfer coefficient in the tube can be quoted from the steady state results although their problem was intrinsically transient.

Due to economic and safety considerations, water is frequently used as a transfer fluid in most low temperature thermal energy storage systems. Therefore, a physical model using water as a transfer fluid will be investigated by a conjugate analytical method rather than a numerical method. The convective heat transfer inside the tube is assumed to be in the thermal entry region, but the velocity field is assumed to be fully developed. The heat transfer in the PCM region and the convection inside the tube are solved simultaneously. The necessity of conjugate analysis under the influence of different parameters is also discussed.

## 2. PHYSICAL MODEL

The melting of the PCM and the tube-side convection in a thermal storage system is an unsteady 2D problem. In order to solve this problem, the following assumptions are necessary.

(1) The inlet velocity is fully developed, but heat transfer occurs in the thermal entry region.

(2) Axial conduction of the transfer fluid is neglected.

(3) The quasi-steady assumption is applied to convective heat transfer inside the tube. Therefore, the temperature distribution of the transfer fluid only depend on the boundary conditions of the tube but are not affected by the temperature distribution of the transfer fluid at a previous time step. In other words, transient convection in the tube is treated as a series of steady state forced convection problems.

(4) Melting of the PCM in the thermal energy storage system is a 2D problem. Since the variation of the container wall temperature along the axial direction is not very significant, axial conduction in the PCM is neglected.

(5) The initial temperature is assumed to be at the freezing temperature of the PCM (no subcooling).

(6) Since the thickness of the container wall is usually very thin, the heat capacity and axial conduction of the container wall is neglected. Therefore, heat conduction in the container wall is treated as a steady state 1D problem along the radial direction.

Using the above assumptions, forced convection in the tube can be treated as a series of steady state forced convection problems. The equations and boundary conditions governing incompressible laminar flow with no viscous dissipation in the tube are as follows [11]:

$$u = 2U_m\left(1-\frac{r^2}{r_i^2}\right) \tag{1}$$

$$u\frac{\partial T_f^0}{\partial x} = \alpha_f\frac{1}{r}\frac{\partial}{\partial r}\left(r\frac{\partial T_f^0}{\partial r}\right) \tag{2}$$

$$T_f^0 = T_i^0 \quad x = 0 \tag{3}$$

$$T_f^0 = T_w^0 \quad r = r_i. \tag{4}$$

The melting of the PCM can be treated as a series of 1D melting problems along the radial direction. Therefore, the energy equation for the PCM and the boundary conditions are

$$\frac{\partial T_p^0}{\partial t} = \alpha_p\frac{1}{r}\frac{\partial}{\partial r}\left(r\frac{\partial T_p^0}{\partial r}\right) \tag{5}$$

$$k_p r_w\frac{\partial T_p^0}{\partial r} = -\frac{T_b^0 - T_{wo}^0}{\frac{1}{hr_i}+\frac{1}{k_w}\ln\left(\frac{r_w}{r_i}\right)} \quad r = r_w \tag{6}$$

$$T_p^0 = T_m^0 \quad r = s < r_o \tag{7}$$

$$-k_p\frac{\partial T_p^0}{\partial r} = \rho H\frac{ds}{dt} \quad r = s < r_o \tag{8}$$

$$\frac{\partial T_p^0}{\partial r} = 0 \quad r = s = r_o. \tag{9}$$

The relations between the inner surface temperature of the container wall $T_w$ and the outer surface temperature of the container wall $T_{wo}$ will be

$$hr_i(T_b^0 - T_w^0) = \frac{k_w(T_w^0 - T_{wo}^0)}{\ln(r_w/r_i)}. \tag{10}$$

By defining the following dimensionless variables:

$$\left.\begin{aligned} X &= \frac{x}{D} \quad R = \frac{r}{r_i} \quad S = \frac{s}{r_i} \quad R_w = \frac{r_w}{r_i} \quad R_o = \frac{r_o}{r_i} \\ Fo &= \frac{\alpha_p t}{r_i^2} \quad K_w = \frac{k_w}{k_p} \quad K_f = \frac{k_f}{k_p} \quad Pe = \frac{U_m D}{\alpha_f} \\ Ste &= \frac{c_p(T_{in}^0 - T_m^0)}{H} \quad T = \frac{T^0 - T_m^0}{T_{in}^0 - T_m^0} \end{aligned}\right\} \tag{11}$$

the governing equations become:

$$(1-R^2)\frac{\partial T_f}{\partial X} = \frac{2}{Pe}\frac{1}{R}\frac{\partial}{\partial R}\left(R\frac{\partial T_f}{\partial R}\right) \tag{12}$$

$$T = T_w(X) \quad R = 1 \tag{13}$$

$$T = 1 \quad X = 0 \tag{14}$$

$$\frac{\partial T_p}{\partial Fo} = \frac{1}{R}\frac{\partial}{\partial R}\left(R\frac{\partial T_p}{\partial R}\right) \tag{15}$$

$$\frac{\partial T_p}{\partial R} = -\frac{T_b - T_{wo}}{\frac{R_w}{K_f Nu}+\frac{R_w\ln R_w}{K_w}} \quad R = R_w \tag{16}$$

$$T_p = 0 \quad R = S < R_o \tag{17}$$

$$\frac{dS}{dFo} = -Ste\frac{\partial T_p}{\partial R} \quad R = S < R_o \tag{18}$$

$$\frac{\partial T_p}{\partial R} = 0 \quad R = S = R_o \tag{19}$$

$$K_f Nu(T_b - T_w) = \frac{K_w(T_w - T_{wo})}{\ln R_w}. \quad (20)$$

## 3. SOLUTIONS

### 3.1. *Forced convection in the tube*

Forced convective heat transfer in the tube result in neither constant wall temperature nor constant heat flux boundary conditions. It should instead be treated as a forced convection problem with an arbitrarily varied wall temperature. The inlet temperature of the thermal energy storage system is $T_{in} = 1$ and the wall temperature varied ($T_{w,1}$ at $X = 0$). Therefore, the wall temperature variation at $X = 0$ is $\Delta T_{w,1} = T_{w,1} - 1$, and the container wall temperature varies along the axial direction continuously. The full length of the tube is divided into $N$ sections. Therefore, it is assumed that every section has a uniform temperature. In other words, the wall temperature variation along the axial direction is treated as discontinuous variations. For example, the dimensionless wall temperature at a section $i$ and $i+1$ are $T_{w,1}$ and $T_{w,i+1}$, respectively, and the wall temperature variation at $X = i \cdot \Delta X$ is $\Delta T_{w,i+1} = T_{w,i+1} - T_{w,i}$. If $N$ is sufficiently large, the wall temperature variation, $\Delta T_{w,i+1}$, at every section will be very small. This model can accurately describe the continuous variation of the container wall temperature.

After the above treatment, the local Nusselt number will be obtained by an analytical method which is described by Kays and Crawford [11]. The final result is rewritten as:

$$Nu(X) = \frac{\sum_{i=1}^{j} \Delta T_{w,i} \sum_{n=0}^{\infty} G_n \exp\left[-\frac{2\lambda_n^2}{Pe}(X-(i-1)\Delta X)\right]}{4\sum_{i=1}^{j} \Delta T_{w,i} \sum_{n=0}^{\infty} \frac{G_n}{\lambda_n^2} \exp\left[-\frac{2\lambda_n^2}{Pe}(X-(i-1)\Delta X)\right]}. \quad (21)$$

The bulk temperature of the transfer fluid is

$$T_b = T_w - 8\sum_{i=1}^{j} \Delta T_{w,i} \sum_{n=0}^{\infty} \frac{G_n}{\lambda_n^2} \times \exp\left[-\frac{2\lambda_n^2}{Pe}(X-(i-1)\Delta X)\right] \quad (22)$$

where the values of constant $G_n$ and eigenvalues $\lambda_n$ can be found in [11], and the value of $j$ in equations (21) and (22) can be determined by

$$j = \text{int}\left(\frac{X}{\Delta X}\right) + 1 \quad (23)$$

where int in equation (23) is an integer function.

### 3.2. *Heat transfer in the PCM*

The full length of the PCM and container wall is divided into $M$ sections. Since the axial conduction in the PCM and container wall has been neglected, the heat transfer in the PCM in every section can be respectively treated as a 1D problem. Due to the existence of an adiabatic outer container wall, melting in the PCM region occurs in a finite region. Thus, the heat transfer in the PCM can be divided into two stages. Before the melting front reaches the adiabatic shell, a melting process occurs in the PCM. After the melting front reaches the adiabatic shell, the melting process ceases, and heat transfer in the PCM becomes a pure heat conduction problem. Heat conduction in the PCM, with and without phase change, can be solved by an integral approximation method.

Since it is assumed that the PCM is not subcooled, the melting of the PCM is a single-phase problem. Therefore, we can assume the temperature distribution in the liquid region of the PCM has a second-order logarithmic function of the form

$$T_p = T_{wo} + \varphi\left[\frac{\ln(R/R_w)}{\ln(S/R_w)}\right] - (T_{wo} + \varphi)\left[\frac{\ln(R/R_w)}{\ln(S/R_w)}\right]^2 \quad (24)$$

where $T_{wo}$ is the outer surface temperature of the container wall. Equation (24) can satisfy equations (16) and (17) automatically, and $\varphi$ can be obtained by differentiating equation (17) [12]:

$$\frac{\partial T_p}{\partial R}\frac{dS}{dFo} + \frac{\partial T_p}{\partial Fo} = 0. \quad (25)$$

Substituting equations (15) and (18) into equation (25), the following expression is obtained:

$$-Ste\left(\frac{\partial T_p}{\partial R}\right)^2 + \frac{1}{R}\frac{\partial}{\partial R}\left(R\frac{\partial T_p}{\partial R}\right) = 0. \quad (26)$$

Substituting equation (24) into equation (26), an expression for $\varphi$ is derived:

$$2T_{wo} + \varphi = \frac{\sqrt{(1+2T_{wo}Ste)} - 1}{Ste}. \quad (27)$$

Substituting equations (24) and (27) into equation (18), the location of the melting front can be expressed as

$$\frac{dS}{dFo} = \frac{\sqrt{(1+2T_{wo}Ste)} - 1}{S\ln(S/R_w)}. \quad (28)$$

Integrating equation (28) in the time interval (0, $Fo$) gives

$$\frac{1}{2}S^2 \ln\frac{S}{R_w} - \frac{1}{4}(S^2 - R_w^2) = \int_0^{Fo} (\sqrt{(1+2T_{wo}Ste)} - 1)\, dFo. \quad (29)$$

The dimensionless temperature gradient at the outer surface of container wall then becomes

$$\left.\frac{\partial T_p}{\partial R}\right|_{R=R_w} = -\frac{1}{R_w \ln(S/R_w)}\left(2T_{wo} - \frac{\sqrt{(1+2T_{wo}Ste)}-1}{Ste}\right). \quad (30)$$

Substituting equation (30) into equation (16), the outer surface temperature of the container wall is obtained.

After the melting front reaches the adiabatic shell, heat transfer in the PCM becomes a pure conduction problem with a boundary condition of the first kind at the inner boundary ($R = R_w$) and an adiabatic boundary condition at the outer boundary ($R = R_o$). Therefore, it can be assumed that the temperature profile in the liquid PCM is as follows:

$$T_p = T_{wo} - 2\eta\left[\frac{\ln(R/R_w)}{\ln(R_o/R_w)}\right] + \eta\left[\frac{\ln(R/R_w)}{\ln(R_o/R_w)}\right]^2. \quad (31)$$

Equation (31) can satisfy the boundary condition at the inner wall and outer wall automatically, and $\eta$ can be obtained from an integral equation. Integrating equation (15) on the interval ($R_w$, $R_o$), and using the boundary conditions, equation (19), the integrated energy equation for the PCM will become

$$\frac{d\Theta}{dFo} = -R_w \left.\frac{\partial T_p}{\partial R}\right|_{R=R_w} \quad (32)$$

where

$$\Theta = \int_{R_w}^{R_o} RT_p \, dR. \quad (33)$$

Substituting equation (31) into equation (32), the following relation for $\eta$ is obtained:

$$\left[\frac{R_o^2 - R_w^2}{4[\ln(R_o/R_w)]^2} - \frac{R_w^2}{2\ln(R_o/R_w)} - \frac{R_o^2}{2}\right] \times \frac{d\eta}{dFo} - \frac{2}{\ln(R_o/R_w)}\eta + \frac{R_o^2 - R_w^2}{2}\frac{dT_{wo}}{dFo} = 0. \quad (34)$$

The initial condition for $\eta$ must satisfy the total sensible heat of PCM varied continually with time. If it can be assumed that the melting front reached the adiabatic shell at $Fo = Fo_o$, the initial value of $\eta$ can be determined by the following equation [12]:

$$\int_{R_w}^{R_o} RT_p(R, Fo_c^-) \, dR = \int_{R_w}^{R_o} RT_p(R, Fo_o^+) \, dR \quad (35)$$

where $T_p(R, Fo_o^-)$ and $T_p(R, Fo_o^+)$ in equation (35) can be calculated by equations (24) and (31), respectively. The temperature gradient at the container wall outer surface is

$$\left.\frac{\partial T_p}{\partial R}\right|_{R=R_w} = -\frac{2\eta}{R_w \ln(R_o/R_w)}. \quad (36)$$

By substituting equation (36) to equation (16), the outer surface temperature of the container wall is obtained.

### 3.3. *Solution procedure*

The calculation is started at $Fo = 0$. For any time step, the problem can be solved by the following procedure:

(1) Guess a distribution of the inner surface temperature of the container wall along the axial direction $T_w(X)$.

(2) Calculate $Nu(x)$ and $T_b(X)$ for different locations of the axial coordinate $X$.

(3) Calculate the distribution of the outer surface temperature of the container wall along axial direction $T_{wo}(X)$ by equation (20).

(4) Calculate the location of the melting front and dimensionless temperature gradient at the outer surface of the container wall for different locations of the axial coordinate $X$.

(5) Solve equations (16) and (20) to obtain the variations of the inner surface temperature of the container wall $T'_w(X)$.

(6) Compare the assumed inner surface temperature of the container wall $T_w(X)$ and the calculated value $T'_w(X)$. If $|T_w(X) - T'_w(X)|_{max} \leqslant 10^{-5}$, calculate the next time step. If not, return to step (1).

During the iteration of $T_w$, underrelaxation is necessary. The underrelaxation factor used is 0.8. The grid size used for the calculation was $N = 50$ and $M = 150$ with the dimensionless time step $\Delta Fo = 0.05$. Calculations using finer grid size ($N = 100$ and $M = 300$) and smaller time step ($\Delta Fo = 0.02$) were also performed for some cases. The melting fronts obtained by finer grids and smaller time steps showed only 0.5% difference compared with present grid size and time step.

## 4. RESULTS AND DISCUSSION

Since paraffins have been widely used in low temperature thermal storage systems, the PCM used in the following calculations is *n*-octadecane. The transfer fluid inside the tube is water, and the container wall is made of metal with a high thermal conductivity ($K_w = 1000$).

Before studying the heat transfer in the thermal energy storage system with conjugate laminar forced convection, the semi-analytical solution is verified by numerical solution. The present authors numerically studied the heat transfer enhancement in latent heat thermal energy storage system by using external radial finned tubes [13]. The structure of the thermal energy storage system studied in [13] was similar to Fig. 1 but external radial fins were added in the PCM region. Melting in the PCM was solved by using a temperature transforming model [14], and the forced convection inside the tube was solved by the same method as the

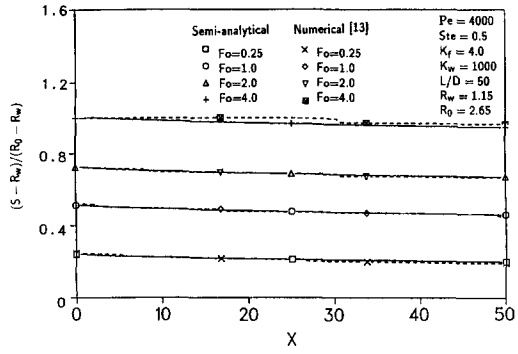


Fig. 2. Comparison of melting fronts obtained by the semi-analytical solution and the numerical solution of [13].

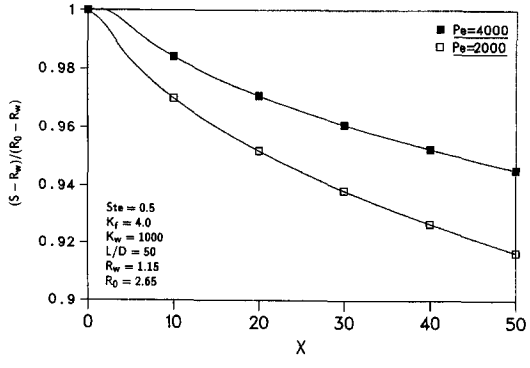


Fig. 3. Melting fronts along the axial direction for different Peclet numbers at $Fo = 4$.

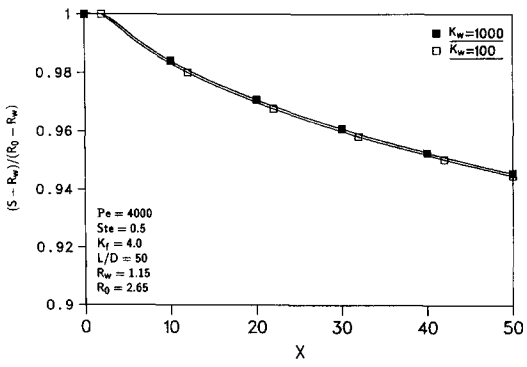


Fig. 4. Melting fronts along the axial direction for different thermal conductivities of the container wall at $Fo = 4$.

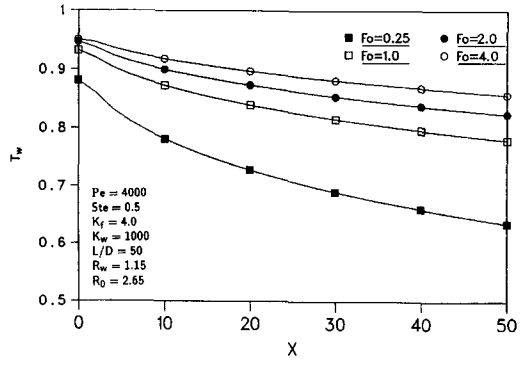


Fig. 5. Inner surface temperature of container wall along axial direction for different Fourier number.

present paper. Figure 2 shows the comparison of the melting front obtained by the present solution and the numerical solution of ref. [13]. Clearly, the differences between the present semi-analytical solution and the numerical solution in ref. [13] are very small, especially for $Fo = 0.25$, 1.0 and 2.0. For $Fo = 4.0$, the radius of the melting front obtained by the present semi-analytical solution is slightly smaller than that obtained by the numerical solution due to the effect of axial conduction, which is not considered in the present paper. However, the difference between the present semi-analytical solution and the numerical solution is very small even for $Fo = 4.0$. Therefore, the assumptions of neglecting the effect of axial in the PCM and container wall are acceptable approximations.

As can be seen from Fig. 2, the melting velocity for a smaller $X$ is faster than the velocity for a larger $X$, because the local Nusselt number and the temperature of the transfer fluid for a smaller $X$ is higher than the value for a larger $X$. For $Fo = 4.0$, the melting front at the entry of the tube reached the outer container wall. However, the variation of melting fronts at different $X$ are not significant. Figure 3 shows the melting fronts for different Peclet numbers at $Fo = 4.0$. With small Peclet numbers, heat transfer to the PCM is much slower as indicated in Fig. 3. The melting fronts for different container wall thermal conductivities are shown in Fig. 4. The effect of thermal resistance in the container wall on the melting front is negligibly small.

Figure 5 shows the variation of the inner surface temperature of the container wall along the axial direction for different Fourier numbers. It can be seen that the temperature decreases along the axial direction. The temperature gradient along the axial direction in the beginning stage is large, but decreases with time. For large Fourier numbers, the decrease in temperature along the axial direction is nearly linear except at the entrance of the tube.

Figures 6–8 show the local Nusselt number along the axial direction for different dimensionless lengths of the tube. Local Nusselt numbers for laminar forced convection under the boundary conditions of Constant Wall Temperature (CWT) and Constant Heat Flux (CHF) are also given in Figs. 6–8 for comparison. The local Nusselt number increases with the Fourier number. For the full length of the tube, the local Nusselt numbers are neither equal to the value for the CWT boundary condition, or to that for the CHF boundary condition. The local Nusselt numbers at the entrance of the tube are close to the values corresponding to CWT. For larger $X$, the local Nusselt numbers approach the value corresponding to CHF. The local Nusselt numbers are closer to the value of the CHF boundary condition for the longer tube.

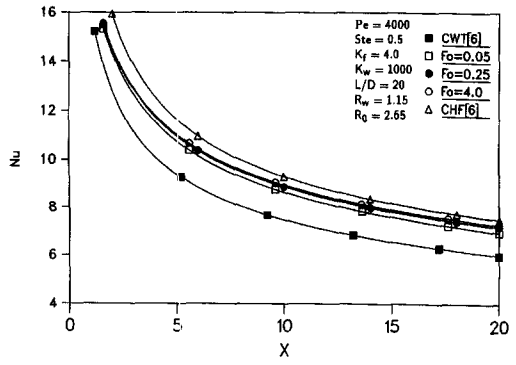


Fig. 6. Local Nusselt numbers along the axial direction for different Fourier numbers ($L/D = 20$).

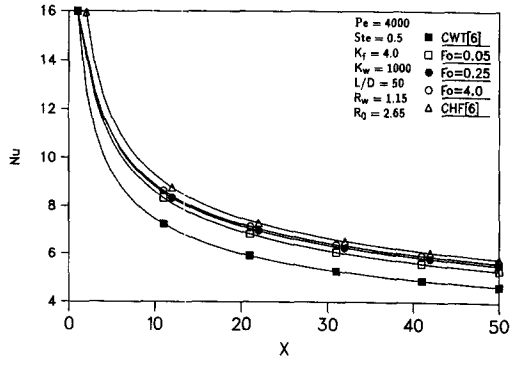


Fig. 7. Local Nusselt numbers along the axial direction for different Fourier numbers ($L/D = 50$).

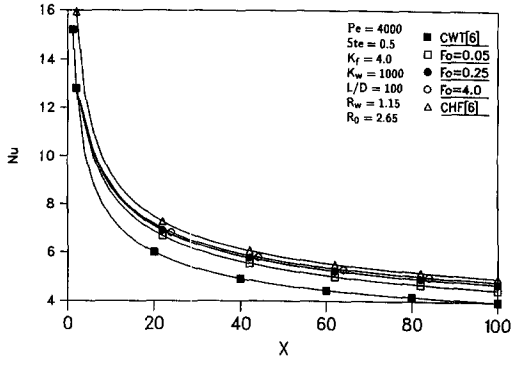


Fig. 8. Local Nusselt numbers along the axial direction for different Fourier numbers ($L/D = 100$).

Also, at the end of the tube for $L/D = 100$, the heat transfer still has not reached a thermally fully developed state. Therefore, if the fully developed Nusselt correlation was used to calculate the heat transfer from the transfer fluid to the container wall, a significant error would be introduced.

Bellecci and Conti [9] have calculated similar problems numerically in order to check Cao and Faghri's [7] conclusions. However, a liquid metal was used as the transfer fluid. According to Bellecci and Conti's [9] results for the thermal and velocity developing state described by Cao and Faghri [7], the local Nusselt number can be calculated by steady state numerical results under the CHF boundary condition [10], even though their problem was intrinsically transient. As can be seen from Fig. 8, the local Nusselt numbers are closer to the values associated with the CHF boundary condition for the dimensionless length of the tube $L/D = 100$. This means that for the very long tube ($L/D \geqslant 100$), the local Nusselt number predicted by the present model will approach the local Nusselt number quoted from steady state numerical results. However, a much longer tube will be meaningless for practical applications. Therefore, for thermal energy storage systems with laminar forced convection, if a fluid with moderate Prandtl number, such as water, is used as the transfer fluid, the local Nusselt number should be calculated by the present simplified analytical model, or by Cao and Faghri's numerical model [7] which accounts for the thermal development region.

## 5. CONCLUSIONS

A thermal energy storage system with the configuration shown in Fig. 1 has been studied semi-analytically. The transfer fluid and the PCM studied were water and paraffin respectively, since these are prevalent in engineering applications. The results show that convective heat transfer inside the tube never reached the fully developed state, even for a very long tube ($L/D = 100$). The local Nusselt number can not be accurately calculated using correlations for the thermal entry region under CHF boundary conditions, except for very long tubes ($L/D \geqslant 100$). Therefore, the laminar forced convective heat transfer from a transfer fluid of moderate Prandtl number must be solved as a conjugate problem with the change of phase of the PCM.

## REFERENCES

1. C. F. Hsu and E. M. Sparrow, A closed form analytical solution for freezing adjacent to a plane wall cooled by forced convection, *J. Heat Transfer* **103**(3), 596–598 (1981).
2. E. M. Sparrow and C. F. Hsu, Analysis of two-dimensional freezing outside a coolant-carrying tube, *Int. J. Heat Mass Transfer* **24**(8), 1345–1356 (1981).
3. N. Shamsundar, Formulae for freezing outside a circular tube with axial variation of coolant temperature, *Int. J. Heat Mass Transfer* **25**(10), 1614–1616 (1982).
4. N. Shamsundar and E. Rooz, Numerical methods for moving boundary problems. In *Handbook of Numerical Heat Transfer* (Edited by W. J. Minkowycz *et al.*), pp. 747–786. Wiley, New York (1988).
5. Ch. Charach, Y. Keizman and M. Sokolov, Small Stanton number axisymmetric freezing around a coolant-carrying tube, *Int. Commun. Heat Mass Transfer* **18**(5), 639–657 (1991).
6. A. D. Solomon, M. D. Morris, J. Martin and M. Olszewski, The development of a simulation code for a latent heat thermal energy storage system in a space station, Technical Report ORNL-6213 (1986).
7. Y. Cao and A. Faghri, Performance characteristics of a thermal energy storage module : a transient PCM/forced

convection conjugate analysis, *Int. J. Heat Mass Transfer* **34**(1), 93–101 (1991).
8. Y. Cao and A. Faghri, A study of thermal energy storage system with conjugate turbulent forced convection, *ASME J. Heat Transfer* **114**(1), 1019–1027 (1992).
9. C. Bellecci and M. Conti, Phase change thermal storage: transient behavior analysis of a solar receiver–storage module using the enthalpy method, *Int. J. Heat Mass Transfer* **36**(8), 2157–2163 (1993).
10. C. J. Chen and J. S. Chiou, Laminar and turbulent heat transfer in the pipe entrance region for liquid metals, *Int. J. Heat Mass Transfer* **24**(7), 1179–1189 (1981).
11. W. M. Kays and M. E. Crawford, *Convective Heat and Mass Transfer* (2nd Edn). McGraw-Hill, New York (1980).
12. M. N. Ozisik, *Heat Conduction*. Wiley-Interscience, New York (1980).
13. Y. Zhang and A. Faghri, Heat transfer enhancement in latent heat thermal energy storage system by using the external radial finned tube, *J. Enhanced Heat Transfer* (submitted).
14. Y. Cao and A. Faghri, A numerical analysis of phase change problems including natural convection, *ASME J. Heat Transfer* **112**(3), 812–816 (1990).